Efficient bidirectional optical harmonics generation in three-dimensional photonic crystals

Irina V. Soboleva,[1,2,*] Sergey A. Seregin,[1] Andrey A. Fedyanin,[1] and Oleg A. Aktsipetrov[1]

[1]*Faculty of Physics, Lomonosov Moscow State University, 119991 Moscow, Russia*
[2]*A. N. Frumkin Institute of Physical Chemistry and Electrochemistry, Russian Academy of Sciences, 119991 Moscow, Russia*
**Corresponding author: soboleva@nanolab.phys.msu.ru*

Received February 22, 2011; revised May 11, 2011; accepted May 12, 2011; posted May 12, 2011 (Doc. ID 143018); published June 14, 2011

Noncollinear generation of second and third harmonics in three-dimensional photonic crystals of artificial opals is experimentally realized and interpreted in terms of nonlinear diffraction. A factor-of-two enhancement of second- and third-harmonic generation intensity in diffraction maxima directions is observed due to effective phase matching provided by photonic crystal periodicity. Bidirectional diffraction of third harmonics at crystallographic planes (111) and $(\bar{1}11)$ is observed. The broadening of nonspecular diffraction peaks is found to correspond to the polycrystalline structure of the opal samples. © 2011 Optical Society of America

OCIS codes: 190.2620, 230.5298, 050.5298.

1. INTRODUCTION

Nonlinear diffraction in media with modified dispersion law attracts high interest because of the possibility to efficiently control the propagation and generation of light. It is defined as the diffraction of optical harmonic radiation at angles of incidence for which the nonlinear Bragg's law is satisfied [1]. The phenomenon of nonlinear diffraction was first shown in the NaH_4Cl multidomain sample with periodic spatial modulation of nonlinear susceptibility, where effective second-harmonic generation (SHG) in noncollinear directions was observed [1]. Subsequently, the same effect was theoretically predicted [2] and experimentally demonstrated [3] in two- and three-dimensional (3D) nonlinear photonic crystals with periodic alternation of quadratic susceptibility. Efficient generation of noncollinear harmonics in nonlinear photonic crystals caused by nonlinear diffraction of light allows one to consider them as a new type of nonlinear crystals for multibeam and multifrequency harmonics generation. Nonlinear diffraction in nonlinear photonic crystals has been observed in the narrow angular range around the collinear direction due to large period and small reciprocal vector in comparison with the light wave vector. The study of nonlinear diffraction is of interest in materials where the opposite case—the wave vector length equals or is smaller than the reciprocal vector length—is realized. The nonlinear diffraction in these structures is expected to be essentially noncollinear. Three-dimensional photonic crystals (PCs) of artificial opals are an example of such materials. They possess well-studied optical properties such as photonic bandgap [4], Bragg diffraction [5], and Fano-type resonances in transmission spectra [6]. They also can lead to new materials with a photonic bandgap tunable under the impact of external fields by its filling with functional materials such as semiconductors, ferroelectrics, and magnetics [7–9]. Three-dimensional photonic crystals of opals are also of interest for a number of nonlinear optical applications as was recently demonstrated for collinear SHG and third-harmonic generation (THG) [10–12].

In this paper, the noncollinear configuration of nonlinear diffraction of second (SH) and third harmonics (TH) in 3D photonic crystals of artificial opals is realized. Generally, the directions for efficient diffraction in periodic media are determined by Bragg law for wave vector mismatch $\Delta\mathbf{k}$ in the reciprocal space

$$\Delta\mathbf{k} = \mathbf{k}_{\text{out}} - \mathbf{k}_{\text{in}} = \mathbf{G}, \tag{1}$$

where $\mathbf{k}_{\text{in}}$ and $\mathbf{k}_{\text{out}}$ are wave vectors of incident and diffracted waves and $\mathbf{G}$ is the reciprocal vector of the structure. This can be generalized for optical harmonics generation by introducing the wave vector mismatch $\Delta\mathbf{k}_{\text{NL}} = \mathbf{k}_{\text{out}}^{n\omega} - n\mathbf{k}_{\text{in}}^{\omega}$ between wave vectors of fundamental, $\mathbf{k}_{\text{in}}^{\omega}$, and nth-order harmonic, $\mathbf{k}_{\text{out}}^{n\omega}$, [1]. Equation (1) can be solved graphically using Ewald construction [2] similar to the sketch shown in Fig. 1(a). The sketch represents the part of the cross section of the opal Brillouin zone with the $(\bar{1}\,\bar{1}1)$ plane corresponding to the plane of incidence in reciprocal space [4]. The (111) surface corresponds to the growth surface. Bragg law is satisfied if $\mathbf{k}_{\text{in}}$, $\mathbf{k}_{\text{out}}$, and $\mathbf{G}_{111}$ form the triangle of quasi-phase matching. The triangle is isosceles for linear diffraction and the angles of incidence and diffraction, θ_{in} and θ_{dif}, are equal. This is not the case for nonlinear diffraction as there is a phase mismatch caused by dispersion of refractive index of the sample. Though nonlinear processes in photonic crystals are conventionally described by the effective refractive index approximation [11,13], the triangles method in reciprocal space avoids complex calculations of effective refractive index and determines the shape and position of diffracted peaks with enough accuracy.

2. EXPERIMENT

Samples of artificial opals were prepared by natural sedimentation of silica microspheres [14]. The opal surface coincides with the growth (111) plane except for a slight slant due to surface polishing. The period of the opal structure, $d =$

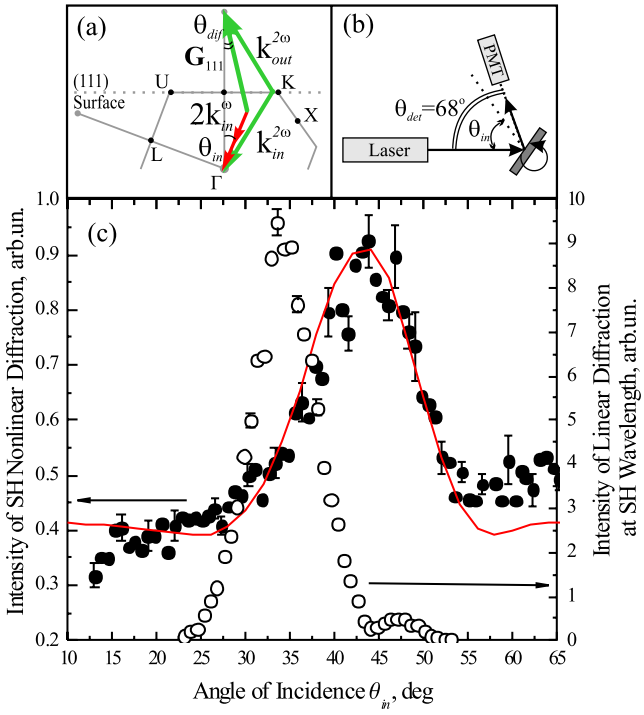

Fig. 1. (Color online) (a) Scheme of linear (large arrows, green online) and nonlinear (small arrows, red online) diffraction at second-harmonic frequency in opal PCs shown in reciprocal space. (b) Principal scheme of the nonlinear diffraction experiment: the incident wave is p-polarized, while the polarization state of the diffracted wave is not controlled. (c) The angular spectra of nonlinear diffraction of second-harmonic (filled circles) and of linear diffraction of frequency-doubled YAG laser radiation (open circles) in the opal photonic crystal.

205 nm, is estimated from the spectral position of the stop band in transmission spectra. Immersion of the opals in ethanol (refractive index of $n = 1.36$ at 532 nm) was used to reduce the influence of Rayleigh scattering at the opal packing defects.

Nonlinear diffraction of second and third harmonics in opals was realized by k-domain spectroscopy when the angle of incidence was varied while the fundamental wavelength was fixed. The 1064 nm output of the YAG:Nd^{3+} laser with pulse duration of 10 ns, energy of 6 mJ per pulse, and spot diameter of 1 mm was used as fundamental radiation. In the nonlinear case, $\theta_{in} \neq \theta_{dif}$ and the experimental configuration was chosen to be able to separately measure angular dependences of the nonlinear signal on the angle of incidence θ_{in} and on the angle of detection $\theta_{det} \equiv \theta_{in} + \theta_{dif}$ between the wave vector of fundamental radiation and detecting direction while θ_{in} was fixed. Two experimental schemes were realized, as shown in Fig. 1(b): measurements of indicatrix of nonlinear signal $I_{nw}(\theta_{det})$ for fixed θ_{in} and angular dependences $I_{nw}(\theta_{in})$ for fixed θ_{det}. In the second-harmonic diffraction experiments, the θ_{det} value was fixed to 68°.

3. SECOND-HARMONIC NONLINEAR DIFFRACTION

The angular spectrum of nonlinear diffraction of second harmonics is shown in Fig. 1(c), with the angular spectrum of linear diffraction of frequency-doubled YAG laser radiation for comparison. Intensity of the linear diffraction of SH light is peaked in the specular direction. The only peak close to the specular direction is observed for nonlinear diffraction as the length of reciprocal vector $G_{111} \equiv 2\pi/d$ is close to $2k_{2\omega}$. The SH diffraction peak is shifted to larger values of incident angles in comparison with linear diffraction maximum because $2k_{\omega} < k_{2\omega}$ due to normal dispersion of silica. Enhancement of the SH intensity is about two times in comparison with the SHG signal out of the diffraction peak. Despite the fact that the opal is macroscopically centrosymmetrical, SHG is possible at the microspheres' surfaces due to inverse symmetry breaking [10,15]. SHG enhancement in the nonlinear diffraction peak area is caused by quasi-phase matching of fundamental and harmonic waves involving reciprocal vector G_{111}. A difference between the angular positions of the two peaks argues that nonlinear diffraction is not a cascade process of second-harmonic generation and its further diffraction, and has to be considered as a single process. The angular dependence of SH nonlinear diffraction has a peak at $\theta_{in} = 44°$ with the half-width at half-maximum (HWHM) $\Delta\theta_{NL} = 5.5° \pm 0.3°$. Recently, SHG enhancement was observed in the specular direction at the photonic bandgap edge in one-dimensional (1D) and 3D photonic crystals [10,16–21] and at the microcavity mode of 1D photonic crystals [22–24]. The SHG enhancement in 1D photonic crystals is associated with quasi-phase matching condition fulfillment due to the media periodicity. In 3D photonic crystals, the SHG peak observed in the specular direction can be considered as the −1st order of nonlinear diffraction due to nonlinear Bragg law satisfaction.

The peak of nonlinear diffraction is widened in comparison with the linear diffraction peak. The broadening $W_{SH} = \Delta\theta_{NL}/\Delta\theta_L = 1.55 \pm 0.05$ is caused by different values for the refractive indices and absorbance coefficients of fundamental and SH waves. The shape of the SH diffraction peak, caused by phase matching of fundamental and harmonic waves, is described by the phase-mismatching factor $F(\theta) \sim \mathrm{sinc}^2[(\Delta\mathbf{k}_{NL}(\theta) - \mathbf{G}_{111})L/2]$, where L is interaction length [25]. The fit of the experimental spectrum with the $F(\theta_{in})$ dependence is shown in Fig. 1(c) by the solid curve. The values for the opal effective refractive indices, n_{ω} at 1064 nm and $n_{2\omega}$ at 532 nm, are obtained as the average indices of the spheres and voids of the opal, taking into account that the spheres have pore structure and form the close-packed fcc structure in opal [26]:

$$n = [0.54n_{SiO_2}^2 + 0.2n_{air}^2 + 0.26n_{eth}^2]^{1/2}, \quad (2)$$

where n_{SiO_2}, n_{air}, n_{eth} are the refractive indices of silica, air, and ethanol, respectively. The obtained values of $n_{\omega} = 1.34$ and $n_{2\omega} = 1.35$ are in good agreement with $n_{2\omega} = 1.345$ as determined from transmission spectral measurements. The interaction length achieved in the fit of the SH diffraction peak with $F(\theta_{in})$ is $L \sim 4.5\,\mu$m, which corresponds to 20 layers of opal sample. A small L value in comparison with sample thickness can be the result of a large amount of defects in the opal packing. Rayleigh scattering at the defects leads to fundamental-wave weakening into the incident direction, broadening of the diffraction cone, and a decrease in effective interaction length.

4. MULTIDIRECTIONAL THIRD-HARMONIC NONLINEAR DIFFRACTION

The multidirectional nonlinear diffraction can be observed if the wave vectors are long enough, i.e., $\mathbf{k} \sim \mathbf{G}$. In this case, two triangles are enclosed simultaneously, involving two reciprocal vectors, for example, $\mathbf{G}_{111}$ and $\mathbf{G}_{\bar{1}11}$ as shown in Fig. 2(a). This leads to coincidence of two dips corresponding to two PBG in transmission spectra of opal [27] and simultaneous observation of two orders of diffraction (the 0th and the −1st) in reflectance. The multidirectional nonlinear diffraction can be observed in both second- and third-harmonics generation, but in the structures studied here, this situation is realized for the TH nonlinear diffraction only. As the angle of incidence θ_{in} is fixed at 68°, while θ_{det} is changed from 20° to 200° [inset in Fig. 2(b)], simultaneous TH nonlinear diffraction at two symmetry planes, (111) and $(\bar{1}\,11)$, can be realized in opal with a lattice period of 205 nm and fundamental wavelength of 1064 nm.

The indicatrix of third-harmonic nonlinear diffraction is shown in Fig. 2(b). The indicatrix of linear diffraction of frequency-tripled YAG laser radiation is also shown for comparison. The indicatrix of third-harmonic nonlinear diffraction intensity has two peaks at $\theta_{\text{det}} = 62°$ and $\theta_{\text{det}} = 163°$ with HWHM $\Delta\theta_{\text{NL},\bar{1}11} = 36° \pm 3°$ and $\Delta\theta_{\text{NL},111} = 12° \pm 1°$, respectively. The TH diffraction peak at $\theta_{\text{det}} = 163°$ involves the reciprocal vector $\mathbf{G}_{111}$. It is almost specular and is shifted from the peak of linear diffraction because of the difference between $\mathbf{k}_{3\omega}$ and $3\mathbf{k}_{\omega}$. This is shown in Fig. 2(a) as a non-

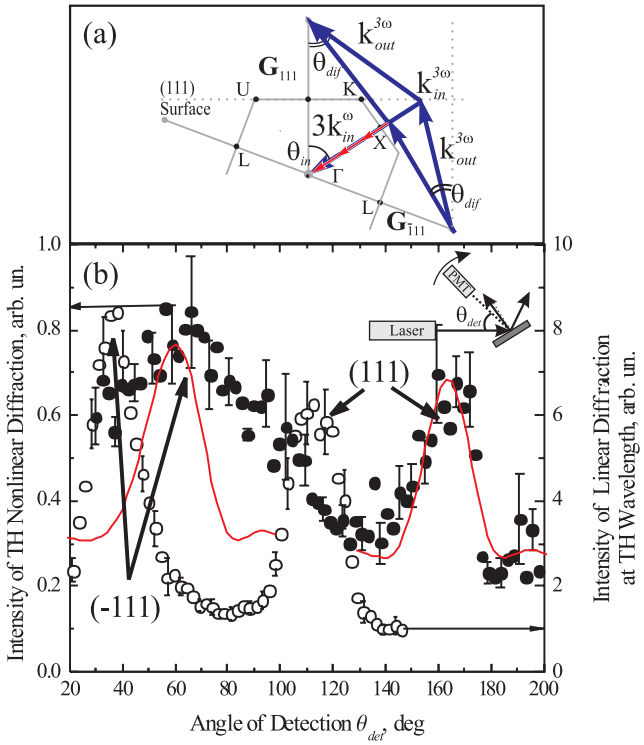

Fig. 2. (Color online) (a) Scheme of bidirectional linear (dark, blue online) and nonlinear light, (red online) diffraction at third-harmonic frequency in the reciprocal space. (b) The angular spectra of nonlinear diffraction of third-harmonic (filled circles) and of linear diffraction of frequency-doubled YAG laser radiation (open circles) in the opal photonic crystal. (Inset) The scheme of the experiment: the incident wave is *p*-polarized, and the polarization state of diffracted wave is not controlled.

isosceles triangle with different angles for $\mathbf{k}_{\omega}^{\text{in}}$ and $\mathbf{k}_{3\omega}^{\text{out}}$ due to dispersion of the effective refractive index of the opal sample. The TH diffraction peak at $\theta_{\text{det}} = 62°$ is caused by nonlinear diffraction at the series of $(\bar{1}\,11)$ planes that corresponds to the bottom triangle in Fig. 2(a).

The TH diffraction peaks are widened in comparison with linear diffraction. The broadening of the peak observed at $\theta_{\text{det}} = 163°$ is $W_{\text{TH},111} = \Delta\theta_{\text{NL}}/\Delta\theta_{L} = 1.42 \pm 0.04$, and that of the small-angle peak is $W_{\text{TH},\bar{1}11} = 3.89 \pm 0.15$. The $W_{\text{TH},111}$ value is close to W_{SH}, while $W_{\text{TH},\bar{1}11}$ is much larger. The fit of both peaks by angular dependences of phase mismatch factor $F(\theta_{\text{det}})$ with $L = 1.0\,\mu$m and effective refractive indices of $n_{\omega} = 1.34$ and $n_{3\omega} = 1.37$ calculated using Eq. (2) is shown in Fig. 2(b) by solid curves. The fitting of the large-angle peak has good agreement with the experiment, while the width of left peak appears to be approximately three times larger.

5. ROLE OF STRUCTURE DEFECTS IN TIRD-HARMONIC DIFFRACTION PEAK BROADENING

The reason for the large width of TH diffraction peaks should be looked for in the opal structure. Artificial opals formed by natural sedimentation technique have a polycrystalline structure with a typical domain lateral size of 50 to 100 μm and thickness of 10 to 20 μm [28]. Thickness of domains is small in comparison with the the lateral size because the main type of defect in opals is stacking faults in the layer sequence along the growth axis such as ABCABABC, while the fcc lattice is characterized by the ABCABC sequence. The polycrystalline structure of the sample surface leads to slight misorientation of local normals to the domain surfaces in comparison with the normal to the macroscopic sample surface. Recently, the enhancement of second and third-harmonics generation was shown to be enabled in disordered polydomain structures. Random modulation of nonlinear susceptibilities leads to formation of a continuous domain of the reciprocal vectors $\mathbf{G}$ and fulfillment of the phase-matching conditions becomes possible for a wide range of incident angles and wavelength of the fundamental wave [29,30]. The set of local [111] directions and corresponding $\mathbf{G}_{111}$ reciprocal vectors forms the bodily cone around the growth axis of opal. The probability of existence of a domain with the certain reciprocal vector $\mathbf{G}_{111}$ different from the growth axis orientation has an angular distribution close to Gaussian with the maximum along the growth direction. The shape of spectral features such as the dip in transmittance or the peak in reflectance is an envelope function of the diffraction maxima at this set of domains. The width of the envelope function is the measure of a domain's misorientation in the sample and, consequently, of the defect density. Coherent Bragg diffraction at the set of polycrystals leads to essential broadening of features in the transmission spectra of artificial opals [28].

The polycrystalline structure of opals leads to the fulfilment of the Bragg law (1) at different incident angles in the domains with local normals differently oriented to the surfaces. The effective Bragg diffraction in opals is observed in some range of incident angles determined by the width of bodily cone formed by the local normals. As the result, two diffraction orders are observed simultaneously for several incident angles. Figures 3(a) and 3(b) show linear and nonlinear TH diffraction indicatrices for incident angles of $\theta_{\text{in}} = 60°$, 68°, and 76°. The

series demonstrates different ratios of intensity of two peaks for different angles of incidence. There is only a small-angle peak corresponding to diffraction at $(\bar{1}\,11)$ planes at $\theta_{in} = 60°$, the small-angle peak at $\theta_{in} = 68°$ is more intensive than the large-angle peak corresponding to diffraction at growth (111) planes, and the large-angle peak at $\theta_{in} = 76°$ is more intensive than the small-angle one. Intensities of the diffraction maxima are correlated with the number of opal domains involved in the diffraction process. The deviation of domain normal from the growth axis decreases the diffraction intensity. The θ_{in} range, where Bragg law (1) is satisfied for both (111) and $(\bar{1}\,11)$ planes, is estimated as 10° centered at 68°. Figure 3 shows that the widths of small- and large-angle maxima are different for both nonlinear and linear diffraction. The broadening in the linear case is attributed to different sizes of domains in the (111) and $(\bar{1}\,11)$ planes. Because the lateral size of the opal domains is larger than the thickness, the effective domain lateral size for the $(\bar{1}\,11)$ planes is 3 to 5 times smaller, and the corresponding bodily cone is 3 to 5 times wider, than for the (111) planes. This is caused by the fact that the stacking faults maintaining the order of packing in the (111) planes break it in the $(\bar{1}\,11)$ planes, making the size of domains in the $(\bar{1}\,11)$ planes effectively smaller. Thus the width of the TH-diffraction small-angle peak is due to the interplay between natural nonlinear broadening that is associated with dispersion of material and additional broadening that is associated with the increased density of defects in the $(\bar{1}\,11)$ planes in comparison with the (111) planes. The other reason for broadening of the large-angle edge of the nonlinear diffraction peak at the $(\bar{1}\,11)$ planes is linear diffraction at the (111) planes. The TH radiation that is nonlinearly diffracted at the $(\bar{1}\,11)$ planes is scattered at the packing defects. The TH light scattered at the large angle appears in the direction of the effective linear diffraction at the (111) planes, and diffracts. The width of this peak added to the original nonlinear diffraction peak produces the broadening of the resulting peak. Scattering makes the conditions favorable for the TH light generated during the nonlinear diffraction process to diffract in all three possible directions, i.e., that of the linear and nonlinear $(\bar{1}\,11)$ diffraction and of the linear (111) diffraction; the intensity of the TH signal is determined by the scattering cross section in these directions.

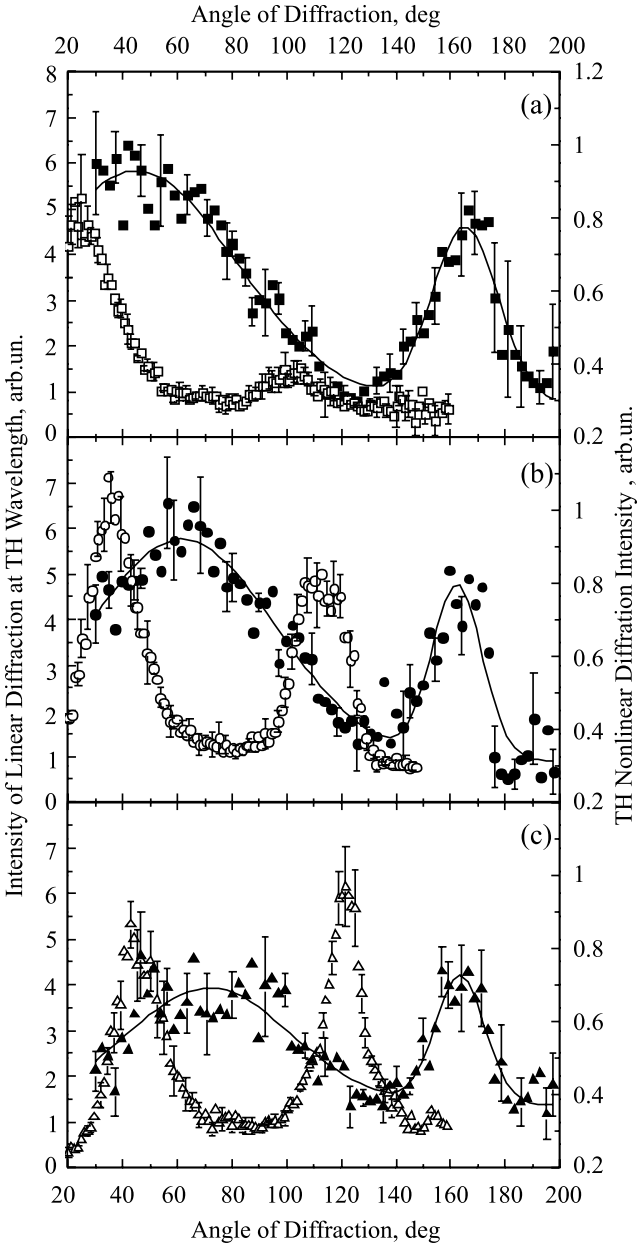

Fig. 3. (a) Indicatrix of linear (open squares) and nonlinear diffraction (filled squares) at TH wavelength for 60° angle of incidence. (b) Indicatrix of linear (open circles) and nonlinear diffraction (filled circles) at TH wavelength for 68° angle of incidence. (c) Indicatrix of linear (open triangles) and nonlinear diffraction (filled triangles) at TH wavelength for angle of incidence of 76°. Solid curves show the fit of the experimental data, with a double-peak Gaussian line shape.

6. CONCLUSIONS

In conclusion, multidirectional nonlinear diffraction of second and third harmonics in 3D photonic crystals of artificial opals involving $\mathbf{G}_{111}$ and $\mathbf{G}_{\bar{1}11}$ reciprocal vectors is studied. The factor-of-two enhancement of second- and third-harmonic generation in the directions of the diffraction maxima is observed due to effective phase matching imposed by the photonic crystal periodicity. The bidirectional diffraction of the third harmonics observed is due to the three-dimensionality of opal photonic crystals at the (111) and $(\bar{1}\,11)$ crystallographic planes. The peak of nonlinear diffraction at the $(\bar{1}\,11)$ planes is essentially nonspecular and widened in comparison with the peak diffracted at the (111) planes that is attributed to the polycrystalline structure of opal samples. The diffractive properties of 3D photonic crystals of opal may be important for application in nanophotonics, integrated optics, and nanoelectronics. Infiltration of opal voids with liquids or polymers with high nonlinearity provides a way to obtain new bidirectional nonlinear crystals with operating frequencies in the IR, visible, and UV ranges. The use of the nonspecular diffractive peak allows study of the properties of materials infiltrated in opal voids, such as for ferroelectrics and semiconductors, independent of the surface influence.

ACKNOWLEDGMENTS

This work is supported by the Russian Foundation for Basic Research (RFBR) and the Russian Ministry of Education and Science.

REFERENCES

1. I. Freund, "Nonlinear diffraction," Phys. Rev. Lett. **21**, 1404–1406 (1968).
2. V. Berger, "Nonlinear photonic crystals," Phys. Rev. Lett. **81**, 4136–4139 (1998).
3. L.-H. Peng, C.-C. Hsu, and Y.-C. Shih, "Second-harmonic green generation from two-dimensional $\chi^{(2)}$ nonlinear photonic crystal with orthorhombic lattice structure," Appl. Phys. Lett. **83**, 3447–3449 (2003).
4. A. V. Baryshev, A. A. Kaplyansky, V. A. Kosobukin, M. F. Limonov, and A. P. Skvortsov, "Spectroscopy of the photonic stop band in synthetic opals," Phys. Solid State **46**, 1331–1339 (2004).
5. A. V. Baryshev, A. A. Kaplyansky, V. A. Kosobukin, M. F. Limonov, K. B. Samusev, and D. E. Usvyat, "Bragg diffraction of light in synthetic opals," Phys. Solid State **45**, 459–471 (2003).
6. M. V. Rybin, A. B. Khanikaev, M. Inoue, K. B. Samusev, M. J. Steel, G. Yushin, and M. F. Limonov, "Fano resonance between Mie and Bragg scattering in photonic crystals," Phys. Rev. Lett. **103**, 023901 (2009).
7. M. Ajgaonkar, Y. Zhang, H. Grebel, and C. W. White, "Nonlinear optical properties of a coherent array of submicron SiO_2 spheres (opal) embedded with Si nanoparticles," Appl. Phys. Lett. **75**, 1532–1534 (1999).
8. R. Fujikawa, A. V. Baryshev, A. B. Khanikaev, J. Kim, H. Uchida, and M. Inoue, "Enhancement of Faraday rotation in 3D/Bi:YIG/1D photonic heterostructures," J. Mater. Sci.: Mater. Electron. **20**, 493–497 (2008).
9. K. Napolskii, N. Sapoletova, A. Eliseev, G. Tsirlina, A. Rubacheva, E. Ganshina, M. Kuznetsov, M. Ivanov, V. Valdner, E. Mishina, A. van Etteger, and Th. Rasing, "Magnetophotonic properties of inverse magnetic metal opals," J. Magn. Magn. Mater. **321**, 833–835 (2009).
10. A. A. Fedyanin, O. A. Aktsipetrov, D. A. Kurdyukov, V. G. Golubev, and M. Inoue, "Nonlinear diffraction and second-harmonic generation enhancement in silicon-opal photonic crystals," Appl. Phys. Lett. **87**, 151111 (2005).
11. P. P. Markowicz, H. Tiryaki, H. Pudavar, and P. N. Prasad, "Dramatic enhancement of third-harmonic generation in three-dimensional photonic crystals," Phys. Rev. Lett. **92**, 083903 (2004).
12. M. Botey, M. Maymó, A. Molinos-Gómez, L. Dorado, R. A. Depine, G. Lozano, A. Mihi, H. Míguez, and J. Martorell, "Light generation at the anomalous dispersion high energy range of a nonlinear opal film," Opt. Express **17**, 12210–12216 (2009).
13. M. Centini, C. Sibilia, M. Scalora, G. D'Aguanno, M. Bertolotti, M. J. Bloemer, C. M. Bowden, and I. Nefedov, "Dispersive properties of finite, one-dimensional photonic band gap structures: Applications to nonlinear quadratic interactions," Phys. Rev. E **60**, 4891–4898 (1999).
14. V. N. Bogomolov, S. V. Gaponenko, I. N. Germanenko, A. M. Kapitonov, E. P. Petrov, N. V. Gaponenko, A. V. Prokofiev, A. N. Ponyavina, N. I. Silvanovich, and S. M. Samoilovich, "Photonic band gap phenomenon and optical properties of artificial opals," Phys. Rev. E **55**, 7619–7625 (1997).
15. J. Martorell, "Parametric nonlinear interaction in centrosymmetric three-dimensional photonic crystals," J. Opt. Soc. Am. B **19**, 2075–2082 (2002).
16. J. Martorell, R. Vilaseca, and R. Corbalán, "Second harmonic generation in a photonic crystal," Appl. Phys. Lett. **70**, 702–704 (1997).
17. A. V. Balakin, V. A. Bushuev, N. I. Koroteev, B. I. Mantsyzov, I. A. Ozheredov, A. P. Shkurinov, D. Boucher, and P. Masselin, "Enhancement of second-harmonic generation with femtosecond laser pulses near the photonic band edge for different polarizations of incident light," Opt. Lett. **24**, 793–795 (1999).
18. T. V. Dolgova, A. I. Maidikovskii, M. G. Martem'yanov, G. Marovsky, G. Mattei, D. Schuhmacher, V. A. Yakovlev, A. A. Fedyanin, and O. A. Aktsipetrov, "Giant second harmonic generation in microcavities based on porous silicon photonic crystals," JETP Lett. **73**, 6–9 (2001).
19. T. V. Dolgova, A. I. Maidykovski, M. G. Martemyanov, A. A. Fedyanin, O. A. Aktsipetrov, G. Marowsky, V. A. Yakovlev, and G. Mattei, "Giant microcavity enhancement of second-harmonic generation in all-silicon photonic crystals," Appl. Phys. Lett. **81**, 2725–2727 (2002).
20. M. Maymó, J. Martorell, A. Molinos-Gómez, and F. López-Calahorra, "Visible second-harmonic light generated from a self-organized centrosymmetric lattice of nanospheres," Opt. Express **14**, 2864–2872 (2006).
21. I. V. Soboleva, E. M. Murchikova, A. A. Fedyanin, and O. A. Aktsipetrov, "Second- and third-harmonic generation in birefringent photonic crystals and microcavities based on anisotropic porous silicon," Appl. Phys. Lett. **87**, 241110 (2005).
22. T. V. Dolgova, A. I. Maidykovski, M. G. Martemyanov, A. A. Fedyanin, O. A. Aktsipetrov, G. Marowsky, V. A. Yakovlev, G. Mattei, N. Ohta, and S. Nakabayashi, "Giant optical second-harmonic generation in single and coupled microcavities formed from one-dimensional photonic crystals," J. Opt. Soc. Am. B **19**, 2129–2140 (2002).
23. T. V. Murzina, R. V. Kapra, T. V. Dolgova, A. A. Fedyanin, O. A. Aktsipetrov, K. Nishimura, H. Uchida, and M. Inoue, "Magnetization-induced second-harmonic generation in magnetophotonic crystals," Phys. Rev. B **70**, 012407 (2004).
24. O. A. Aktsipetrov, T. V. Dolgova, A. A. Fedyanin, T. V. Murzina, M. Inoue, K. Nishimura, and H. Uchida, "Magnetization-induced second- and third-harmonic generation in magnetophotonic crystals," J. Opt. Soc. Am. B **22**, 176–186 (2005).
25. Y. R. Shen, *The Principles of Nonlinear Optics* (Wiley, 1984).
26. I. I. Bardyshev, A. D. Mokrushin, A. A. Pribylov, E. N. Samarov, V. M. Masalov, I. A. Karpov, and G. A. Emelchenko, "Porous structure of synthetic opals," Colloid J. **68**, 20–25 (2006).
27. A. V. Baryshev, A. B. Khanikaev, H. Uchida, M. Inoue, and M. F. Limonov, "Interaction of polarized light with three-dimensional opal-based photonic crystals," Phys. Rev. B **73**, 033103 (2006).
28. V. N. Astratov, A. M. Adawi, S. Fricker, M. S. Skolnick, D. M. Whittaker, and P. N. Pusey, "Interplay of order and disorder in the optical properties of opal photonic crystals," Phys. Rev. B **66**, 165215 (2002).
29. W. Wang, K. Kalinowski, V. Roppo, Y. Sheng, K. Koynov, Y. Kong, C. Cojocaru, J. Trull, R. Vilaseca, and W. Krolikowski, "Second- and third-harmonic parametric scattering in disordered quadratic media," J. Phys. B, At. Mol. Opt. Phys. **43**, 215404 (2010).
30. V. Roppo, W. Wang, K. Kalinowski, Y. Kong, C. Cojocaru, J. Trull, R. Vilaseca, M. Scalora, W. Krolikowski, and Yu. Kivshar, "The role of ferroelectric domain structure in second harmonic generation in random quadratic media," Opt. Express **18**, 4012–4022 (2010).